Spatial Information Research (2026) 34:50
https://doi.org/10.1007/s41324-026-00704-w

CASE REPORT

Chlorophyll-*a* and phytoplankton community responses to cyclone Dana in the coastal waters of the north-western Bay of Bengal

Amit Kumar Jena[1] · Kamal Kumar Barik[2] · Sumit Kumar Mohanty[2,3] · Suchismita Sahu[2] · Suchismita Srichandan[3] · Sanjiba Kumar Baliarsingh[4] · Alakes Samanta[4] · Pratap Kumar Chhotaray[2] · Sudheer Joseph[4] · T. M. Balakrishnan Nair[4]

Received: 8 June 2026 / Revised: 11 July 2026 / Accepted: 24 July 2026

Abstract
This study examines the imprint of cyclone Dana on chlorophyll-*a* (chl-*a*) variability in the coastal waters of the north-western Bay of Bengal. In situ observations and satellite/model-derived biophysical parameters were combined to characterize the upper-ocean responses. Dana exhibited a low translational speed during its intense phase, which amplified the Ekman Pumping Velocity, promoting upwelling of cooler, nutrient-rich sub-surface water. This fertilization produced approximately a two-fold increase in chl-*a* concentrations after the cyclone, accompanied by a sea surface temperature drop of about 2.2 °C indicative of vertical mixing and upwelling. Phytoplankton abundance rose in the post-cyclone phase, although diatoms dominated throughout. A synthesis of previous Bay of Bengal cyclones confirmed a multifold post-cyclone rise in chl-*a*. These findings highlight the influence of low translational speed in modulating cyclone-driven biophysical coupling within tropical coastal ecosystems.

Keywords Tropical cyclone · Translational speed · Ekman pumping velocity · Phytoplankton · Sea surface temperature

1 Introduction

Phytoplankton play a pivotal role in marine ecosystems, serving as primary producers that sustain the food chain up to the top trophic levels, such as large fish [1]. Phytoplankton ecology is largely controlled by ambient water quality, including nutrient availability, water column transparency, and other factors. Therefore, variations in phytoplankton communities can reveal significant changes in water quality and nutrient availability, acting as indicators of ecological stress from issues such as eutrophication, algal blooms, and climate change [2]. Additionally, monitoring these patterns is crucial for managing fisheries, predicting algal blooms, ecosystem trophodynamics, and understanding global carbon cycling [2, 3]. Thus, consistent phytoplankton monitoring aids in better coastal management and helps devise strategies to protect marine biodiversity and support the livelihoods of human populations dependent on these ecosystems.

The Bay of Bengal (BoB) is a semi-enclosed basin in the north Indian Ocean. This Bay experiences seasonally reversing tropical monsoon patterns, with precipitation exceeding evaporation [4]. The large volume of fluvial inflow from several Indian rivers into the BoB led to surface salinization due to the formation of a thick barrier layer [5]. The north-western BoB receives a large volume of riverine inflow from major rivers such as the Ganga, Brahmaputra, Mahanadi, and Godavari, which enhances phytoplankton productivity, especially in coastal waters [6]. In the context of the phytoplankton community and biomass, this region experiences seasonal blooms, mostly during the pre-southwest monsoon and after its withdrawal [7]. Amongst several pockets of the north-western BoB, the coastal waters

✉ Suchismita Srichandan
suchismita.sima@gmail.com

1 Indian Institute of Technology Bombay, Mumbai 400076, India

2 Centurion University of Technology and Management, Bhubaneswar, Odisha, India

3 Department of Marine Sciences, Berhampur University, Bhanja Bihar, Brahmapur 760007, India

4 Indian National Centre for Ocean Information Services, Ministry of Earth Sciences, Government of India, Hyderabad 500090, India

Published online: 12 August 2026

of Odisha (an Indian state bordering the western BoB) have been reported with several algal blooms and exhibit a long-term bimodal pattern in the distribution of phytoplankton biomass (proxy: chlorophyll-*a*, hereafter chl-*a*) with a primary peak during pre-southwest monsoon and a secondary during post-southwest monsoon [8].

Apart from the general physical forcing that is mostly driven by reversing monsoons and boundary currents (in this case, East India Coastal Current), extreme events such as tropical cyclones exert a significant impact on the regional biogeochemistry, especially phytoplankton ecology, being the first respondents to such events [9]. It's important to mention here that the north-western BoB on the east coast of India is one of the hotspots of cyclone landfall. Tropical cyclones are the most catastrophic natural disasters, driving vigorous upper-ocean mixing, leading to upwelling and nutrient entrainment into the upper light zone, and resulting in an increase in phytoplankton production [10–12].

In particular, the biophysical response to the cyclone is controlled by cyclone intensity, Ekman pumping velocity, translational speed, and subsurface oceanic conditions [13, 14]. Cyclone-induced vertical mixing and upwelling elevate surface chl-*a* levels by transporting nutrients to the upper layers [15, 16]. Primary production is further increased by nutrient enrichment from terrestrial sources, which is facilitated by excessive rainfall and freshwater runoff [17, 18].

In the recent past, a severe cyclonic storm, "Dana," brewed in the BoB and made landfall near Bhitarkanika and Dhamra Port region on the east coast of India on 25 October 2024 (Fig. 1). The coastal waters of these regions of the north-western BoB are ecological-economical hotspots owing to the effect of major river estuaries, pronounced capture fisheries, migratory sea turtles' mating grounds, etc. [19, 20]. Against this backdrop, this study was undertaken in the coastal waters of the north-western BoB to decipher the effect of cyclone Dana on the variability of biophysical parameters, with special reference to phytoplankton ecology.

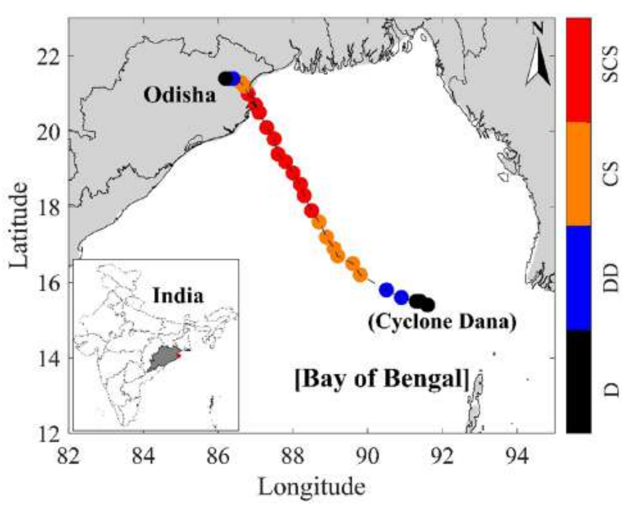

Fig. 1 Geographic location of the study area and the best-track trajectory of Tropical Cyclone Dana in the Bay of Bengal. Coloured markers represent the cyclone intensity at successive positions according to the India Meteorological Department (IMD) classification, illustrating its progression from Depression (D) to Deep Depression (DD), Cyclonic Storm (CS), and Severe Cyclonic Storm (SCS) before landfall along the Odisha coast

Although these studies have collectively established the general pathway linking cyclone-induced mixing, upwelling, nutrient entrainment, and chl-*a* enhancement in the BoB, several aspects of this response remain inadequately resolved for the north-western coastal sector. Much of the available evidence derives from satellite observations, which are frequently interrupted by dense cloud cover during and immediately after cyclone passage, and which are further biased in the optically complex, river-influenced waters of this region. Rapid-response field measurements acquired at the immediate landfall zone across the pre- and post-cyclone phases, therefore, remain scarce. Moreover, most reports emphasize chl-*a* as a proxy of phytoplankton biomass, whereas the accompanying shifts in phytoplankton abundance and taxonomic composition, together with their propagation to higher trophic levels, are rarely documented for a single event. The relative role of translational speed, as independent of peak intensity, in governing the magnitude of the biological response also remains insufficiently constrained for the BoB. The present study addresses these gaps by combining rapid-response in situ observations with satellite and model-derived biophysical fields to resolve how the low translational speed of cyclone Dana modulated Ekman-driven upwelling and the coupled responses of chl-*a*, phytoplankton community, and higher-trophic response, and by placing this event within a regional synthesis of BoB cyclones.

2 Materials and methods

2.1 Study area, cyclone Dana, and pre-survey background

The BoB, located in the northeastern Indian Ocean, borders India, Bangladesh, Myanmar, and Sri Lanka. This semi-enclosed basin is characterized by complex oceanographic features, making it a critical region for studying physical, chemical, and biogeochemical processes influenced by monsoonal dynamics and terrestrial runoff [21]. The coastal waters of the BoB exhibit distinct physical, chemical, and biogeochemical attributes influenced by its dynamic interactions with rivers, monsoons, and anthropogenic activities. Physically, the region is characterized by high freshwater input from major rivers like the Ganges, Brahmaputra, and Irrawaddy, resulting in strong salinity gradients and stratification, especially during the monsoon season [22]. Nutrient dynamics, particularly nitrogen and phosphorus, drive primary productivity and contribute to seasonal hypoxia in certain areas. The interactions between nutrient loading, organic matter decomposition, and microbial activity further shape its biogeochemical environment, influencing ecosystem health and marine biodiversity [23]. In general, tropical cyclones are known to affect the coastal waters of the western BoB through changes in biogeochemistry and increases in chl-*a*, and sometimes leading to higher fisheries productivity [17, 24].

Tropical cyclone Dana formed in the BoB as a low-pressure area on 20 October 2024. It moved nearly north-northwestwards and intensified into a depression over east central BoB on 22 October 2024. Subsequently, within 4 days of its formation, it became a severe cyclonic storm. As per the cyclone forecast by the Indian Meteorological Department (IMD), regarding its landfall on the east coast of India close to the Bhitarkanika and Dhamara region of Odisha, field surveys were conducted in the near-coastal waters of Kendrapara District (Pentha) and Bhadrak District (Dhamara) on 23 October 2024 (Fig. 1). Cyclone Dana crossed the north Odisha coast close to Habalikhati (Bhitarkanika) and Dhamra Port on 25 October 2024 as a severe cyclonic storm. After the passage of the cyclone, again, field surveys were conducted on 29 October 2024 and 9 November 2024 (Fig. 1).

2.2 Methodology-in situ data

Water samples were collected from two stations in the coastal waters of the study area to analyze different water quality parameters. To estimate the chl-*a*, surface seawater samples were collected and subsequently filtered onto GF/F filter paper, extracted in 90% acetone, and measured spectrophotometrically using a UV–Visible spectrophotometer (Make: Shimadzu, Model: UV-2600) by following the standard protocol [25]. For the measurement of Coloured Dissolved Organic Matter (CDOM), seawater samples were filtered through 0.22 µm membrane filters and measured using a spectrophotometer (Make: Shimadzu, Model: UV-2600) following Kowalczuk and Kaczmarek (1996) [26]. One liter of surface seawater sample was collected and preserved with fixatives (Lugol's iodine solution and 3% neutralized formaldehyde) for phytoplankton taxonomy. In the laboratory, qualitative and quantitative estimations were carried out by following standard identification keys [27].

2.3 Methodology-satellite/model data

The cyclone track information, maximum sustained wind speed, and translational speed of cyclone Dana were obtained from the IMD best track data [28] and IMD reports [29]. The daily chl-*a* concentrations with 4 km spatial resolution were retrieved from the Moderate Resolution Imaging Spectroradiometer-Aqua (MODISA) satellite [30]. The daily chl-*a* climatology was calculated using available cloud-free data for 2002–2024. The daily Sea Surface Temperature (SST) was obtained from the Group for High Resolution Sea Surface Temperature (GHRSST) with a spatial resolution of 0.01 Decimal Degrees [31, 32]. The daily wind components were retrieved from EOS06/Oceansat-3 Scatterometer [33]. Ekman components were derived using the Scatterometer wind fields as per the following

$$\text{Ekmanzonalmasstransport}\,(\text{Mx}) = \frac{\tau_y}{f} \quad (1)$$

$$\text{Ekmanmeridionalmasstransport}\,(\text{My}) = -\frac{\tau_x}{f} \quad (2)$$

$$\text{EkmanPumpingVelocity}\,(\text{EPV}) = Curl\left(\frac{\tau}{\rho_w f}\right) \quad (3)$$

where τ is wind stress, f is the Coriolis parameter, and ρ_w is the seawater density [34].

3 Results

In the present study, to investigate the effect of cyclone Dana, the temporal evolution of daily SST, SST climatology, daily chl-*a* concentrations, its climatology and, in situ chl-*a* concentrations during the pre-and post-cyclonic phases was analysed (Fig. 2). In general, one of the primary prerequisites for cyclogenesis is the prevalence of SST exceeding ~ 26 °C [35, 36]. In the present study, SST exhibited relatively higher values (~31 °C), which were ~ 1.5 °C above its climatology, indicating conducive conditions for cyclone evolution prior to landfall. After the passage of the cyclone, a notable decline in SST (~2.2 °C) was observed, which signified surface cooling likely driven by enhanced vertical mixing and upwelling in response to the cyclone. During landfall, the SST dropped below its climatological value. As observed in previous cyclones in the BoB, SST normalized to climatological values returned to climatological values within a day. The lower SST indicated mixing in the water column, injecting phytoplankton growth-promoting nutrients into the upper light zone.

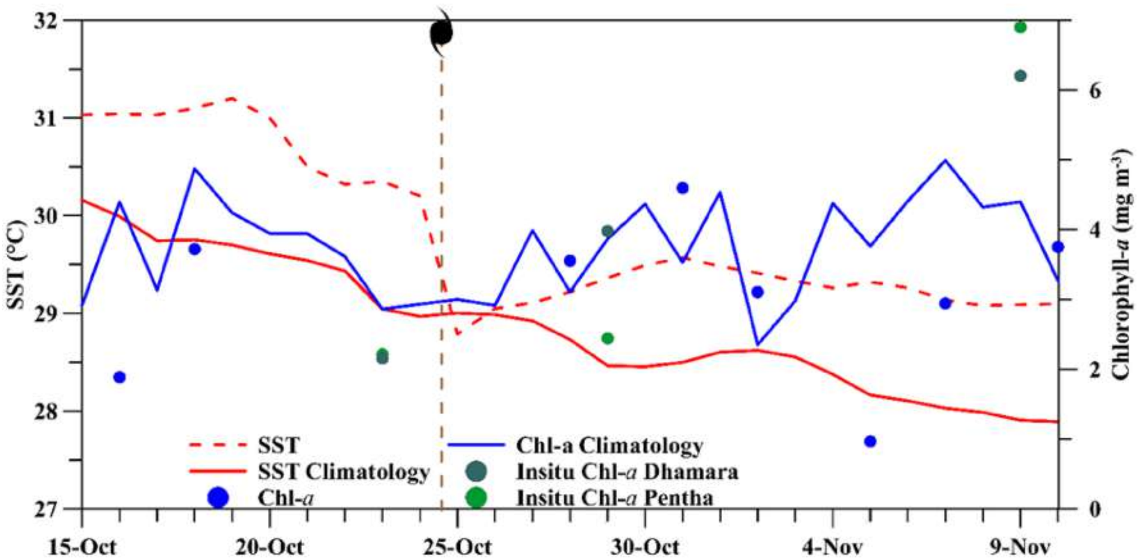

Fig. 2 Temporal variations in satellite-derived chlorophyll-*a* concentration and sea surface temperature (SST) within a 0.5° × 0.5° region (86.9–87.4°E, 20.3–20.8°N) in the Bay of Bengal. Dashed lines represent MODIS-Aqua observations, solid lines indicate climatological means, and coloured circles denote in situ chlorophyll-*a* measurements collected at Dhamara and Pentha. The vertical dashed line marks the landfall of Tropical Cyclone Dana

To decipher the response of cyclone and resultant perturbation in ambient environmental conditions, satellite-retrieved distribution of chl-*a* was investigated. However, given the chl-*a* data gaps, primarily due to limited satellite coverage during intense cloud cover, particularly during and immediately following the cyclone, sporadic in situ observations were carried out at the predicted cyclone landfall location [29]. The comparative analysis of pre (~2.2 mg m^{-3}) and post-cyclone (~4 mg m^{-3}) phase chl-*a* concentration, as revealed from in situ data, discerned a significant rise with ~ twofold increment aftermath of the cyclone (Fig. 2). Moreover, a pronounced upsurge in chl-*a* concentrations was observed subsequently, peaking at 6.8 mg m^{-3} in coastal waters of Dhamara and 6.2 mg m^{-3} in the Pentha region (Fig. 2). While examining satellite data for the wider spatio-temporal analysis, significant data gaps due to cloud cover during cyclone yielded sporadic value without continuity. However, in situ chl-*a* concentration provided comparatively higher values with respect to satellite-retrieved chl-*a* climatology.

Given a prominent cyclone-induced increase in chl-*a* concentration, which suggested possible nutrient entrainment into the surface layers, EPV variability over the bay was investigated. In general, during cyclonic conditions, EPV increases in coherence with the cyclone progression. The resultant churning of the water column introduces subsurface nutrients to the surface [37]. This variability of EPV vis-à-vis cyclone Dana is illustrated in Fig. 3, where positive values denote upwelling and negative values downwelling. As depicted in Fig. 3, a significantly higher EPV ($>4 \times 10^{-4}$ m s^{-1}) can be noticed during the intense period of the cyclone. Specifically, on 23rd October, a dramatic spread of higher EPV was observed over the entire northern BoB.

The spatio-temporal variation of SST during cyclone Dana in the BoB revealed significant cooling patterns driven by the cyclone's passage (Fig. 4). Prior to the cyclone's arrival, elevated SST provided the requisite energy to sustain the preexisting low-pressure area, thereby fueling the intensity of the cyclone. As the cyclone traversed the ocean, its intense, spiralling winds generated a pronounced wind stress curl, invoking EPV that induced upwelling (Fig. 3). This upwelling entrained cooler, nutrient-rich subsurface waters into the euphotic zone, not only a remarkable SST decline in the cyclone's wake but also a significant enhancement in chl-*a*. A significant decline in SST, to 2.5 °C on 25–26 October, was observed following the intense phase of the cyclone on 24th at 18:00 h. However, spatially, the cooling was more prominent on the right side of the cyclone's track, consistent with enhanced wind stress and Ekman dynamics. The cooling signature was observed a day after the passage of cyclone Dana. It can be noted that higher cooling was observed during the cyclone's intense phase. This is in corroboration with the earlier study on cyclone Sidr, which reported a significant increase in chl-*a* by 3 to 10 times on the right side of the cyclone track in the BoB, attributed to cyclone-induced mixing [38].

Tropical cyclones characterized by high maximum sustained wind speeds and low translational velocities often induce profound oceanic responses. Figure 5 shows the

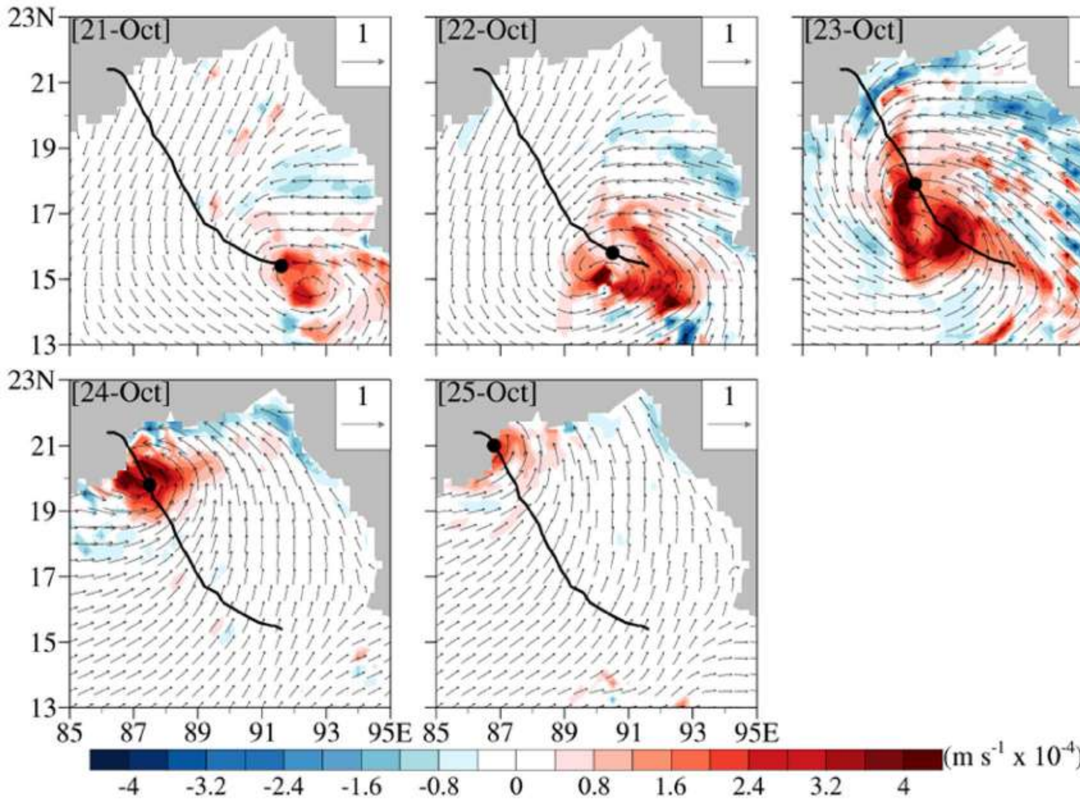

Fig. 3 Spatio-temporal evolution of Ekman pumping velocity (m $s^{-1} \times 10^{-4}$) and surface wind stress during the passage of Tropical Cyclone Dana over the Bay of Bengal (21–25 October 2024). Shaded colours represent Ekman pumping velocity, arrows denote wind stress vectors, the solid black line indicates the cyclone best-track, and the black dot marks the cyclone centre on each day. Landfall occurred along the Odisha coast on 24 October 2024

temporal evolution of maximum sustained wind speed and translational speed during cyclone Dana. The maximum sustained wind speed (60 kt) and low translational speed (10.8 kmph/ 3 m s^{-1}) [39] facilitated vigorous surface churning, resulting in the entrainment of nutrient-rich subsurface waters into the euphotic zone. It moved more slowly than the average translational speed (13.9 kmph) of the cyclone in the BoB during the entire life cycle. The lower translational speed and higher maximum sustained wind speed provided a favourable condition for higher EPV (Fig. 4), strengthening water-column mixing and creating a favourable environment for phytoplankton growth.

The spatial variability of chl-*a* in the BoB after cyclone Dana is shown in Fig. 6, with dates selected based on satellite data availability. The significantly higher values of chl-*a* (>10 mg m^{-3}) can be noticed in the study area (Fig. 6). It is interesting to note that the sequential increment of chl-*a* concentration after the landfall of the cyclone could be due to the availability of nutrients and relatively higher photosynthetic active radiation [14]. Hence, the intensity of tropical cyclones is positively correlated with the post-cyclonic increase in chl-*a* [12, 16]. Another ecological phenomenon, i.e., the prevalence of a large number of jellyfish, was observed along the coast of Dhamara and caught in fishermen's nets. This ancillary information provided evidence supporting high chl-*a* concentration and subsequent development of the food chain. A higher abundance of jellyfish signified a higher zooplankton through a developed food chain.

To investigate the qualitative response of phytoplankton to cyclone Dana, a taxonomic analysis was conducted. It revealed a rise in phytoplankton abundance in the post-cyclone period (avg. 7689 nos/l) in comparison to the pre-cyclone period (avg. 4633 nos/l). Among different phytoplankton groups, diatoms predominated during both the pre- and post-phases of the cyclone. The total phytoplankton abundance values (range 2000 to 16,000 nos/l) are in agreement with the upsurge in phytoplankton biomass (i.e., chl-*a* concentration). The rank order of phytoplankton groups was diatom > dinoflagellate > cyanobacteria during the pre-cyclone phase, whereas two new groups, such as euglenoids and green algae, were observed after the passage of cyclone Dana, and the rank order of phytoplankton groups was as diatom > dinoflagellate > cyanobacteria > euglenoids > green algae. Cyclones often favour the growth of larger phytoplankton groups, such as diatoms,

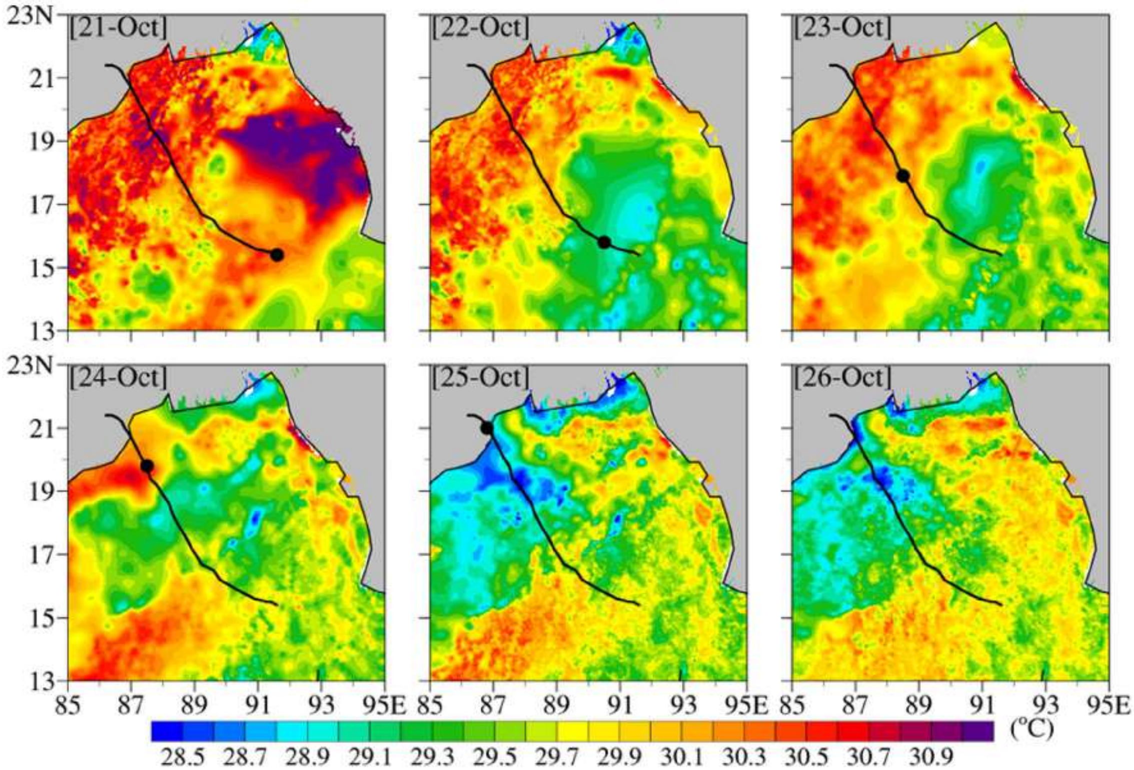

Fig. 4 Daily evolution of sea surface temperature (SST; °C) during the passage of Tropical Cyclone Dana over the Bay of Bengal (21–26 October 2024). Colour shading represents SST, the solid black line indicates the cyclone best-track, and the black dot marks the cyclone centre on each day. The cyclone made landfall along the Odisha coast on 24 October 2024

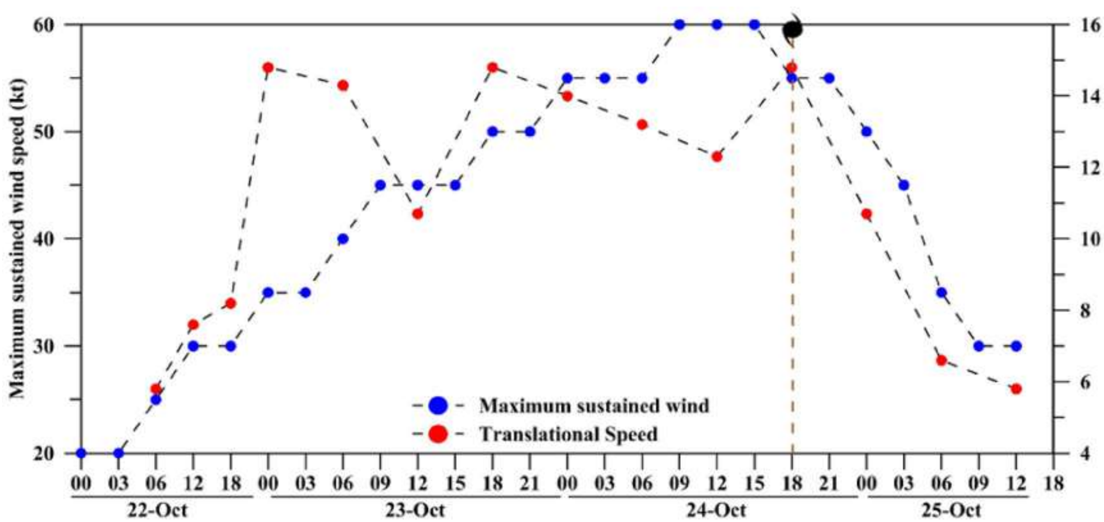

Fig. 5 Temporal evolution of the maximum sustained wind speed (kt) and translational speed (km h^{-1}) of Tropical Cyclone Dana over the Bay of Bengal (22–25 October 2024). The vertical dashed line and cyclone symbol indicate the time of landfall along the Odisha coast

due to the sudden replenishment of the ambient medium with silicate and other nutrients [40]. Conversely, smaller phytoplankton groups, such as cyanobacteria, proliferate under post-cyclone conditions when nutrient levels stabilize [41]. These shifts can impact the entire marine food web and biogeochemical cycling in the region. Cyclones provide excellent opportunities to investigate phytoplankton responses to mesoscale nutrient pulses that are typically not observed in regular monitoring. The peak of phytoplankton abundance likely represents the usual response time of the phytoplankton assemblage to the sudden influx of nutrients caused by the cyclone [42].

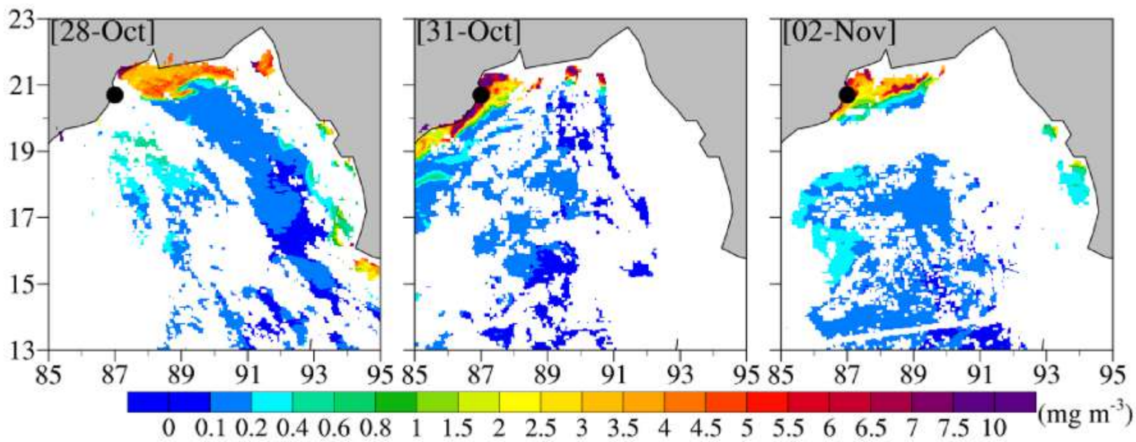

Fig. 6 Spatial distribution of MODIS-Aqua-derived chlorophyll-*a* concentration (mg m^{-3}) following the passage of Tropical Cyclone Dana over the Bay of Bengal. The maps depict the temporal evolution of surface chlorophyll-*a* on 28 October, 31 October, and 2 November 2024, highlighting the post-cyclone biological response. The black dot indicates the cyclone landfall location along the Odisha coast

Another important parameter is CDOM, which more often interferes with the efficient retrieval of chl-*a* from satellites. It revealed no such significant change after the passage of cyclone ($_a$CDOM$_{440}$ 0.18–0.25 m^{-1}) in comparison with the pre-cyclone phase (0.28–0.33 m^{-1}). As there were no significant changes in CDOM magnitude (0.08–0.09 m^{-1}), it can be hypothesized that there was no significant terrigenous influx/river discharge in the coastal waters [43].

4 Discussion

Tropical cyclones in the BoB have been reported to exert significant effects on coastal water quality, especially on the variability of chl-*a*. For instance, cyclone Phailin triggered a significant increase in chl-*a* concentration, particularly in the coastal waters of the north-western BoB [37]. Similarly, cyclone Hudhud also caused a notable upsurge in chl-*a* levels, with the post-cyclone phase witnessing a doubling of concentration in some regions, which persisted for weeks [9]. Another study carried out during cyclone Sidr showed the impact of the extreme event, resulting in a phytoplankton bloom and an enhancement in fishery production after its passage [38]. Beyond enhanced primary production, the biological imprint of such events can propagate through the food web and manifest as conspicuous higher-trophic responses along the coast. A mass jellyfish beaching event was reported along the Puri coast following the landfall of ESCS Mocha [44]. Likewise, widespread fish mortality accompanied by jellyfish beach stranding was documented along the northeastern coast of Odisha following the passage of the VSCS Yaas [45].

To provide a comparative account of the effect of tropical cyclones on the chl-*a* variability, relevant secondary data (literature) were mined for the Indian coastal waters (Table 1). This review revealed that in the Indian Ocean, relatively weaker tropical cyclones can induce intense phytoplankton blooms under favorable conditions, but not all stronger cyclones do. Some parameters like cyclone intensity, translation speed, pre-existing mixed layer depth, and nutricline depth regulate the relationship between the amplitude of chl-*a* concentration and tropical cyclones' effect [12].

As per the available literature, the analysis of cyclone activity and its effects on chl-*a* concentration is detailed in Table 1. Cyclones categorized as Extremely Severe Cyclonic Storms (ESCS) have been observed to influence the coastal water to a maximum extent in terms of an upsurge in chl-*a* concentration, in the aftermath of the cyclone, whereas the Very Severe Cyclonic Storms (VSCS) category has a minimum influence in raising chl-*a* concentration after the passage. Among the ESCS category, cyclone Fani (year 2019) was reported to cause a maximum increase in chl-*a* concentration. In this context, it can be hypothesized that the ESCS category was associated with the highest wind speed and lower translational speed, which could be the major reason behind allowing sufficient time for the extreme event to churn the water column, resulting in a relatively higher degree of nutrient entrainment, thereby boosting chl-*a* after its passage. On the other hand, regarding the VSCS category, for instance, cyclone Okhi, which was associated with high wind speed and translational speed, the chl-*a* signature was less in the aftermath of the cyclone. Furthermore, the Odisha Super Cyclone (1999) recorded a substantial post-cyclone chl-*a* increase to 20 mg m^{-3}, attributed to enhanced nutrient upwelling driven by strong winds and vertical mixing [46]. A relative increase in water column mixing due to the low translation speed of the cyclone is also evident

Table 1 Published records of tropical cyclone-induced changes in sea surface temperature (SST) and chlorophyll-*a* concentration across the Indian seas

Sl No	Cyclone name	Region	Landfall Date (DD-MM-YYYY)	Cyclone Category	Duration (Days)	Pre-cyclone SST (°C)	Post-cyclone SST (°C)	Pre-cyclone Chl-*a* concentration (mg m^{-3})	Post-cyclone Chl-*a* concentration (mg m^{-3})	Translational Speed (m s^{-1})
1	The 1998 Gujarat cyclone	AS	09–06-1998	ESCS	5	31	28	–	–	6.97
2	Odisha Super Cyclone	BoB	29–10-1999	SUCS	5	> 28	22.4	1	20	4.64
3	2000 Tropical Cyclone	BoB	29–11-2000	VSCS	3	28.26	26.18	0.24	1.8	4.6
4	2001 North Indian Cyclone	AS	24–05-2001	ESCS	7	-	< 25	0.1 to 0.4	5 to 8	2.42
5	Sidr	BoB	15–11-2007	VSCS	5	29.46	28.19	0.12	0.3	4.365
6	Nargis	BoB	02–05-2008	VSCS	6	> 30	28.24	–	–	3.30
7	Phyan	AS	11–11-2009	CS	2	29.9	27.9	1	0.45	8.23
8	Phailin	BoB	12–10-2013	VSCS	5	28.46	27.3	0.65	6.16	5.39
9	Hudhud	BoB	12–10-2014	VSCS	5	29.7	27.4	2.28	6.62	4.17
10	Vardah	BoB	12–12-2016	VSCS	5	29	27.8	0.05–0.24	8	3.48
11	Ockhi	AS	01–12-2017	VSCS	8	28.6	26.8	0.29	1.8	4.25
12	Fani	BoB	03–05-2019	ESCS	8	30.4	28.4	0.61	10.93	4.06
13	Amphan	BoB	20–05-2020	SuCS	6	31.55 ± 0.97	28.88 ± 0.58	0.11 ± 0.02	0.64 ± 0.48	3.86
14	Yaas	BoB	26–05-2021	VSCS	3	> 30	27	0.16	0.6	3.03

The table summarizes cyclone name, region, landfall date, India Meteorological Department (IMD) cyclone category, duration, translational speed, pre- and post-cyclone SST and chlorophyll-*a* concentrations, and corresponding references. *Abbreviations: CS* Cyclonic storm, *SCS* Severe cyclonic storm, *VSCS* Very severe cyclonic storm, *ESCS* Extremely severe cyclonic storm, *SuCS* Super cyclonic storm, *BoB* Bay of Bengal, *AS* Arabian sea. The source of information supported by references is provided in the Supplementary Material

from the relatively lower SST in the cyclone category SUCS > ESCS > VSCS.

Taken together, the observations indicate that the biological response to Dana was governed less by peak intensity than by the cyclone's low translational speed, which extended the residence time of wind forcing over the water column and sustained Ekman-driven upwelling. This mechanism links the amplified Ekman Pumping Velocity, the post-cyclone surface cooling, and the approximately two-fold rise in chl-*a* into a single coherent pathway of nutrient entrainment and rapid fertilization. The magnitude of such a response is further modulated by the structure of the upper-ocean mixed layer. A deep upper-ocean mixed layer favours tropical cyclone intensification by maintaining high SSTs and reducing cyclone-induced surface cooling, thereby sustaining ocean-to-atmosphere heat fluxes [47]. The strong winds associated with cyclone passage enhance vertical mixing and entrainment, deepening the mixed layer and thermocline while injecting cold, nutrient-rich subsurface water into the euphotic zone [11, 48]. This nutrient enrichment promotes phytoplankton blooms and the formation or intensification of the deep chlorophyll maximum [49]. In the open ocean, cyclone-induced mixing typically increases the mixed layer depth by 20–30 m, highlighting the significant impact of extreme weather events on upper-ocean physical and biogeochemical processes [50]. Within the shallow, river-influenced waters of the present study, this coupling is reflected in the biological signal recorded after Dana. The concurrent increase in phytoplankton abundance, the persistence of diatom dominance, and the appearance of euglenoids and green algae are consistent with the successional response expected when a pulsed nutrient supply reaches a coastal assemblage. The elevated occurrence of jellyfish along the Dhamara coast further suggests propagation of this pulse through the food web. Such episodic, cyclone-driven productivity events carry implications for regional carbon cycling and fisheries, yet they are poorly resolved by routine monitoring due to their short duration.

Several constraints temper the interpretation of these results and define priorities for future work. The fertilization of the water column was inferred from the coupled response of Ekman Pumping Velocity, surface cooling, and chl-*a* rather than from direct measurement of nutrient concentrations, so the magnitude of nutrient entrainment could not be quantified. Likewise, the pre-cyclone mixed layer depth was not characterized, which limits assessment of how the background stratification modulated the amplitude of the chl-*a* response. In these optically complex, river-influenced coastal waters, satellite retrieval is further affected by coloured dissolved organic matter and by persistent cloud cover during and immediately after the cyclone; this explains the divergence between the sparse satellite values and the higher in situ chl-*a* and constrains the precision of the field record. Direct nutrient sampling, estimation of mixed layer depth from profiling observations, and sustained autonomous monitoring would allow these uncertainties to be resolved and would strengthen the attribution of biological change to cyclone forcing in future events.

5 Conclusion

Cyclone Dana provided an instructive case for examining how a tropical cyclone imprints on phytoplankton biomass and abundance in the coastal waters of the north-western BoB. The dominant control was the cyclone's low translational speed, which prolonged wind forcing over the water column, intensified the Ekman Pumping Velocity, and drove upwelling of nutrient-rich subsurface water into the euphotic zone. This fertilization produced an approximately two-fold post-cyclone rise in chl-*a* and a concurrent increase in phytoplankton abundance, while diatoms retained dominance and two additional groups, euglenoids and green algae, emerged after the cyclone. The comparative synthesis of earlier BoB cyclones reinforced that post-cyclone chl-*a* enhancement is regulated jointly by cyclone intensity, translational speed, and pre-existing ocean conditions rather than by intensity alone. Because satellite retrieval is constrained by persistent cloud cover and adverse weather during such events, sustained in situ capability remains essential. Deployment of autonomous, high-frequency water-quality observatories in these ecologically and economically important waters would provide the uninterrupted records needed to resolve rapid biophysical responses and to advance the ecosystem-based objectives of the United Nations Decade of Ocean Science (2021 to 2030).

Supplementary Information The online version contains supplementary material available at https://doi.org/10.1007/s41324-026-00704-w.

Acknowledgements Authors acknowledge the authorities of their respective organizations for their encouragement in carrying out the present piece of research. Amit Kumar Jena would like to acknowledge the Prime Minister's Research Fellowship (PMRF) and Ocean Engineering Laboratory, Department of Civil Engineering, Indian Institute of Technology Bombay (IITB), for providing facilities for this work. This paper is a part of the doctoral research work of one of the authors (Sumit Kumar Mohanty). This work was carried out as a part of the INCOIS-sponsored research project at the Centurion University of Technology & Management, Bhubaneswar (Grant No INCOIS:F&A:OMAS:2023-26:19). This is INCOIS contribution no. 721.

Author contributions AKJ: Software, Visualization, Validation, Data curation, Formal analysis, Investigation, Writing—original draft; KKB: Conceptualization, Data curation, Formal analysis, Investigation, Writing—original draft; SKM: Investigation; Formal analysis, Validation, Writing—original draft; SS (Suchismita Sahu): Formal analysis, Investigation, Writing—original draft; SS (Suchismita Srichandan): Investigation, Writing—original draft; SKB: Conceptualization, Visualization, Formal analysis; Writing—original draft; AS: Supervision, Resources, Writing—review & editing; PKC: Investigation, Writing—review & editing; SJ: Supervision, Resources, Writing—review & editing; TMB: Supervision, Resources, Writing—review & editing. All authors read and approved the final manuscript.

Funding The funding was provided by Indian National Centre for Ocean Information Services, INCOIS:F&A:OMAS:2023-26:19,Kamal Kumar Barik.

Data availability The datasets used for the aforementioned study are sourced from open-access repositories, and the access links are mentioned in the methodology section. The in-situ data used in this used can be made available upon reasonable request.

Declarations

Conflict of interest The authors declare that they have no known competing financial interests or personal relationships that could have appeared to influence the work reported in this paper.

References

1. D'Costa, P. M., D'Silva, M. S., & Naik, R. K. (2017). Impact of pollution on phytoplankton and implications for marine econiches. In M. Naik & S. Dubey (Eds.), *Marine pollution and microbial remediation* (pp. 205–222). Springer. https://doi.org/10.1007/978-981-10-1044-6_13
2. Sahu, B. K., Pati, P., & Panigrahy, R. C. (2018). Impact of climate change on marine plankton with special reference to Indian Seas. *Indian Journal of Geo Marine Sciences, 47*(02), 259–268.
3. Berdalet, E., Fleming, L. E., Gowen, R., Davidson, K., Hess, P., Backer, L. C., & Enevoldsen, H. (2016). Marine harmful algal blooms, human health and wellbeing: Challenges and opportunities in the 21st century. *Journal of the Marine Biological Association of the United Kingdom, 96*(1), 61–91. https://doi.org/10.1017/S0025315415001733
4. Shenoi, S. S. C., Shankar, D., & Shetye, S. R. (2002). Differences in heat budgets of the near-surface Arabian Sea and Bay of Bengal: Implications for the summer monsoon. *Journal of Geophysical Research: Oceans, 107*(C6), Article 3052. https://doi.org/10.1029/2000JC000679
5. McPhaden, M. J., Foltz, G. R., Lee, T., Murty, V. S. N., Ravichandran, M., Vecchi, G. A., Vialard, J., Wiggert, J. D., & Yu, L. (2009). Ocean-atmosphere interactions during Cyclone Nargis. *EOS, Transactions, American Geophysical Union, 90*(7), 53–60. https://doi.org/10.1029/2009EO070001
6. Seelanki, V., & Pant, V. (2021). An evaluation of the impact of pandemic driven lockdown on the phytoplankton biomass over the North Indian Ocean using observations and model. *Frontiers in Marine Science, 8*, Article 722401. https://doi.org/10.3389/fmars.2021.722401
7. Lotliker, A. A., Baliarsingh, S. K., Sahu, K. C., & Kumar, T. S. (2020). Long-term chlorophyll-a dynamics in tropical coastal waters of the western Bay of Bengal. *Environmental Science and Pollution Research, 27*, 6411–6419. https://doi.org/10.1007/s11356-019-07403-0
8. Raulo, S., Samanta, A., Baliarsingh, S. K., Sarma, V. V. S. S., Joseph, S., Nair, T. B., & Srichandan, S. (2025). Determining chlorophyll-a thresholds for characterizing algal bloom

conditions: An ocean colour remote sensing approach. *Science of the Total Environment, 961*, Article 178353. https://doi.org/10.1016/j.scitotenv.2024.178353

9. Baliarsingh, S. K., Parida, C., Lotliker, A. A., Srichandan, S., Sahu, K. C., & Srinivasa Kumar, T. (2015). Biological implications of cyclone Hudhud in the coastal waters of northwestern Bay of Bengal. *Current Science, 109*(7), 1243–1245.
10. Subrahmanyam, B., Rao, K. H., Srinivasa Rao, N., Murty, V. S. N., & Sharp, R. J. (2002). Influence of a tropical cyclone on chlorophyll-a concentration in the Arabian Sea. *Geophysical Research Letters, 29*(22), Article 2065. https://doi.org/10.1029/2002GL015892
11. Maneesha, K., Murty, V. S. N., Ravichandran, M., Lee, T., Yu, W., & McPhaden, M. J. (2012). Upper ocean variability in the Bay of Bengal during the tropical cyclones Nargis and Laila. *Progress in Oceanography, 106*, 49–61. https://doi.org/10.1016/j.pocean.2012.06.006
12. Chacko, N. (2019). Differential chlorophyll blooms induced by tropical cyclones and their relation to cyclone characteristics and ocean pre-conditions in the Indian Ocean. *Journal of Earth System Science, 128*, 177. https://doi.org/10.1007/s12040-019-1207-5
13. Lin, I., Liu, W. T., Wu, C. C., Wong, G. T., Hu, C., Chen, Z., Liang, W. D., Yang, Y., & Liu, K. K. (2003). New evidence for enhanced ocean primary production triggered by tropical cyclone. *Geophysical Research Letters*. https://doi.org/10.1029/2003GL017141
14. Walker, N. D., Leben, R. R., & Balasubramanian, S. (2005). Hurricane-forced upwelling and chlorophyll *a* enhancement within cold-core cyclones in the Gulf of Mexico. *Geophysical Research Letters, 32*, Article 2005GL023716. https://doi.org/10.1029/2005GL023716
15. Ye, H., Kalhoro, M. A., Sun, J., & Tang, D. (2018). Chlorophyll blooms induced by tropical cyclone Vardah in the Bay of Bengal. *Indian Journal of Geo-Marine Sciences, 47*(07), 1383–1390.
16. Babin, S. M., Carton, J. A., Dickey, T. D., & Wiggert, J. D. (2004). Satellite evidence of hurricane-induced phytoplankton blooms in an oceanic desert. *Journal of Geophysical Research: Oceans, 109*, Article 2003JC001938. https://doi.org/10.1029/2003JC001938
17. Sahoo, S., Baliarsingh, S. K., Lotliker, A. A., Pradhan, U. K., Thomas, C. S., & Sahu, K. C. (2017). Effect of physico-chemical regimes and tropical cyclones on seasonal distribution of chlorophyll-*a* in the Chilika Lagoon, east coast of India. *Environmental Monitoring and Assessment, 189*, 153. https://doi.org/10.1007/s10661-017-5850-5
18. Han, H., Xiao, R., Gao, G., Yin, B., & Liang, S. (2023). Influence of a heavy rainfall event on nutrients and phytoplankton dynamics in a well-mixed semi-enclosed bay. *Journal of Hydrology, 617*, Article 128932. https://doi.org/10.1016/j.jhydrol.2022.128932
19. Pandav, B., & Choudhury, B. C. (2000). Conservation and management of olive ridley sea turtle (*Lepidochelys olivacea*) in Orissa. *Final report: Wildlife Institute of India*.
20. Behera, S., Tripathy, B., Sivakumar, K., Choudhury, B. C., & Pandav, B. (2016). Fisheries impact on breeding of olive ridley turtles (*Lepidochelys olivacea*) along the Gahirmatha coast, Bay of Bengal, Odisha India. *The Herpetological Journal, 26*(2), 93–98.
21. Madhupratap, M., Gauns, M., Ramaiah, N., Kumar, S. P., Muraleedharan, P. M., De Sousa, S. N., Sardessai, S., & Muraleedharan, U. (2003). Biogeochemistry of the Bay of Bengal: Physical, chemical and primary productivity characteristics of the central and western Bay of Bengal during summer monsoon 2001. *Deep Sea Research Part II: Topical Studies in Oceanography, 50*(5), 881–896. https://doi.org/10.1016/S0967-0645(02)00611-2
22. Durand, F., Papa, F., Rahman, A., & Bala, S. K. (2011). Impact of Ganges-Brahmaputra interannual discharge variations on Bay of Bengal salinity and temperature during 1992–1999 period. *Journal of Earth System Science, 120*, 859–872. https://doi.org/10.1007/s12040-011-0118-x
23. Middelburg, J. J., Vlug, T., Jaco, F., & Van der Nat, W. A. (1993). Organic matter mineralization in marine systems. *Global and Planetary Change, 8*(1–2), 47–58. https://doi.org/10.1016/0921-8181(93)90062-S
24. Srichandan, S., Kim, J. Y., Kumar, A., Mishra, D. R., Bhadury, P., Muduli, P. R., Pattnaik, A. K., & Rastogi, G. (2015). Interannual and cyclone-driven variability in phytoplankton communities of a tropical coastal lagoon. *Marine Pollution Bulletin, 101*(1), 39–52. https://doi.org/10.1016/j.marpolbul.2015.11.030
25. Strickland, J. D. H., & Parsons, T. R. (1972). *A practical handbook of seawater analysis*. Fisheries Research Board of Canada. https://doi.org/10.25607/OBP-1791
26. Kowalczuk, P., & Kaczmarek, S. (1996). Analysis of temporal and spatial variability of "yellow substance" absorption in the Southern Baltic. *Oceanologia, 38*(1), 3–32.
27. Tomas, C. R. (1997). *Identifying marine phytoplankton*. Elsevier. https://doi.org/10.1016/B978-0-12-693018-4.X5000-9
28. IMD best track data (2024, November 7). Retrieved November 8, 2024, from https://rsmcnewdelhi.imd.gov.in/
29. IMD Bulletin (2024, October 21). Retrieved November 8, 2024, from https://rsmcnewdelhi.imd.gov.in/download.php?path=uploads%2Farchive%2F1%2F1_ba3068_3.Special+Message+No+3-21Oct2024_1130IST.pdf
30. NASA Ocean Color Web. Retrieved on November 20, 2024, from https://oceancolor.gsfc.nasa.gov/
31. A Group for High Resolution Sea Surface Temperature (GHRSST) data. Retrieved on November 22, 2024, from https://podaac.jpl.nasa.gov/dataset/MUR-JPL-L4-GLOB-v4.1
32. Chin, T. M., Vazquez-Cuervo, J., & Armstrong, E. M. (2017). A multi-scale high-resolution analysis of global sea surface temperature. *Remote Sensing of Environment, 200*, 154–169. https://doi.org/10.1016/j.rse.2017.07.029
33. EOS06/Oceansat-3 Scatterometer wind data. Retrieved November 20, 2024, https://www.mosdac.gov.in/
34. Bhaskar, T. V. S. U., Jayaram, C., Rama Rao, E. P., & Rao, K. H. (2016). Spatio-temporal evolution of chlorophyll-*a* in the Bay of Bengal: A remote sensing and Bio-Argo perspective. *Remote sensing of the oceans and inland waters: Techniques, applications, and challenges* (pp. 171–176). SPIE. https://doi.org/10.1117/12.2223880
35. Gray, W. M. (1968). Global view of the origin of tropical disturbances and storms. *Monthly Weather Review, 96*(10), 669–700.
36. Singh, V. K., & Roxy, M. K. (2022). A review of ocean–atmosphere interactions during tropical cyclones in the North Indian Ocean. *Earth-Science Reviews, 226*, Article 103967. https://doi.org/10.1016/j.earscirev.2022.103967
37. Sarangi, R. K., Mishra, M. K., & Chauhan, P. (2014). Remote sensing observations on impact of Phailin cyclone on phytoplankton distribution in northern Bay of Bengal. *IEEE Journal of Selected Topics in Applied Earth Observations and Remote Sensing, 8*(2), 539–549. https://doi.org/10.1109/JSTARS.2014.2347036
38. Maneesha, K., Sarma, V. V. S. S., Reddy, N. P. C., Sadhuram, Y., Murty, T. R., Sarma, V. V., & Kumar, M. D. (2011). Mesoscale atmospheric events promote phytoplankton blooms in the coastal Bay of Bengal. *Journal of Earth System Science, 120*(4), 773–782. https://doi.org/10.1007/s12040-011-0089-y
39. Banerjee, A., Pattnaik, S., Chakraborty, S., & Vishwakarma, V. (2026). Investigation of unique landfall attributes of cyclone Dana over the Eastern Coast of India: Role of large-scale environment and dry-air intrusion. *Meteorology and Atmospheric Physics, 138*(2), Article 17. https://doi.org/10.1007/s00703-026-01118-x
40. Mangesh, G., Siby, K., Damodar, S. M., Hema, N., & Naqvi, S. W. A. (2016). Cyclone Phyan-induced plankton community

succession in the coastal waters off Goa, India. *Current Science, 111*(6), 1091–1097. https://doi.org/10.18520/cs/v111/i6/1091-1097

41. Thompson, P. A., Paerl, H. W., Campbell, L., Yin, K., & McDonald, K. S. (2023). Tropical cyclones: What are their impacts on phytoplankton ecology? *Journal of Plankton Research, 45*(1), 180–204. https://doi.org/10.1093/plankt/fbac062
42. Zheng, G. M., & Tang, D. (2007). Offshore and nearshore chlorophyll increases induced by typhoon winds and subsequent terrestrial rainwater runoff. *Marine Ecology Progress Series, 333*, 61–74. https://doi.org/10.3354/meps333061
43. Pandi, S. R., Kiran, R., Sarma, N. S., Srikanth, A. S., Sarma, V. V. S. S., Krishna, M. S., Bandyopadhyay, D., Prasad, V. R., Acharyya, T., & Reddy, K. G. (2014). Contrasting phytoplankton community structure and associated light absorption characteristics of the western Bay of Bengal. *Ocean Dynamics, 64*, 89–101. https://doi.org/10.1007/s10236-013-0678-1
44. Jena, A. K., Behera, M. R., Srichandan, S., Baliarsingh, S. K., Mohanty, S., Samanta, A., & Srineash, V. K. (2025). Linking a tropical cyclone and ocean conditions to jellyfish stranding event on the Indian East Coast. *Thalassas: An International Journal of Marine Sciences, 41*(1), Article 47. https://doi.org/10.1007/s41208-025-00802-w
45. Baliarsingh, S. K., Jena, A. K., Srichandan, S., Raulo, S., Joseph, S., Balakrishnan Nair, T. M., & Barik, K. K. (2023). A scientific basis for fish mass mortality and jellyfish beach stranding in relation to cyclone Yaas. *Journal of Coastal Conservation, 27*(2), 15. https://doi.org/10.1007/s11852-023-00944-0
46. Sadhuram, Y. (2004). Record decrease of sea surface temperature following the passage of a super cyclone over the Bay of Bengal. *Current Science, 86*(3), 383–384.
47. Balaguru, K., Chang, P., Saravanan, R., Leung, L. R., Xu, Z., Li, M., & Hsieh, J. S. (2012). Ocean barrier layers' effect on tropical cyclone intensification. *Proceedings of the National Academy of Sciences of the United States of America, 109*(36), 14343–14347. https://doi.org/10.1073/pnas.1201364109
48. Price, J. F. (1981). Upper ocean response to a hurricane. *Journal of Physical Oceanography, 11*(2), 153–175.
49. Jena, A. K., Bhaskar, T. V. S. U., Behera, M. R., Kumar, J. P., & Satish, R. (2025). Investigation of tropical cyclone-triggered upper-oceanic biophysical dynamics in the Bay of Bengal using satellite and BGC-Argo observations during extreme negative IOD event. *International Journal of Remote Sensing*. https://doi.org/10.1080/01431161.2025.2592908
50. Malone, T. C., Pike, S. E., & Conley, D. J. (1993). Transient variations in phytoplankton productivity at the JGOFS Bermuda time series station. *Deep Sea Research Part I: Oceanographic Research Papers, 40*(5), 903–924. https://doi.org/10.1016/0967-0637(93)90080-M